Radical photoinduced cationic frontal polymerization in porous media

Radical Induced Cationic Frontal Photopolymerization in Porous Media

D. Maugeri[1,2], M. Sangermano[2], Y. Leterrier[1*]

(1) Laboratory for Processing of Advanced Composites (LPAC), École Polytechnique Fédérale de Lausanne (EPFL), 1015 Lausanne, Switzerland
(2) Dipartimento di Scienza Applicata e Tecnologia (DISAT), Politecnico di Torino, Torino, Italy

(*) corresponding author

Key-Words: Interpenetrating phase composites; Frontal polymerization; photopolymerization; Epoxy; Polyurethane foam; Aluminum foam

ABSTRACT

Two different interpenetrating phase composites were produced using a radical induced cationic frontal photopolymerization process. The composites were based on a polyurethane (PU) and an aluminum open-cell foams impregnated with a formulation of a cycloaliphatic epoxy with different concentrations of a cationic photoinitiator and a thermal initiator. The influence of both types of initiators on the frontal photopolymerization features was systematically evaluated for the PU foam. It was found to occur only when the concentration of both initiators was greater than 0.5 wt%, leading to full conversion of the epoxy on the whole volume of the 15 mm thick composite samples within less than 100 s. The maximum temperature reached by the propagation front was in the range 275°C-305°C depending on the type of formulation, leading to pores in the epoxy phase and extensive degradation of the PU phase. In the case of the opaque aluminum foam, an additional layer of pure resin was required on the UV exposed surface, which corresponded to a critical mass of few g to ensure sufficient heat generation and trigger the front propagation.

1. INTRODUCTION

Interpenetrating phase composites (IPC) represent an important class of materials with enhanced thermo-mechanical properties compared with their non-IPC analogues [1].

Remarkable synergetic effects include higher stiffness [2] and compressive properties [3] than that of individual components, and advantageous energy absorption capacity [2–4]. The processing of IPC often relies on the infiltration of an open-cell foam preform with a liquid phase, followed by solidification, leading to a co-continuous phase morphology.

Here we report for the first time polymer-polymer and polymer-metal IPC produced using a radical induced cationic frontal photopolymerization (RICFP) process. Frontal polymerization (FP) is one of the most promising alternatives to conventional thermal curing, especially in composite manufacturing, thanks to the very short process time and the ability to maintain high mechanical properties [5,6]. In this method a polymerization front is triggered by a photo-induced activation process and propagates throughout the volume owing to the initial reaction exotherm. It was demonstrated in previous investigations that the front initiates by the dissociation of a radical thermal initiator promoted by the heat released during surface UV-initiated cationic ring-opening polymerization [5–9]. Subsequently, the carbon-centered radicals are oxidized to carbocations by the presence of the iodonium salt towards a radical induced cationic mechanism [10]. Various FP approaches are available depending on the nature of the external stimulus and the type of initiators [11]. The RICFP process is expected to enable a much shorter cycle time (minutes) hence considerably reduced energy requirements over conventional processes (hours), and is particularly interesting to photo-polymerize oligomers within opaque media such as composites and foams. However, a number of drawbacks may limit the applicability of this novel method. Firstly, the reaction exothermicity may induce thermal degradation and boiling of the resin, leading to property degradation and risk of porosity within the final product [12]. Indeed, the ability to sustain a heat-front is strongly dependent on the heat dissipation of the material [13], and temperatures as high as 300°C were reported in case of epoxy resins [10]. In addition, in the case of impregnated foams, interfacial adhesion between the two constituents may be compromised by polymerization shrinkage and thermal contraction during cool-down.

Focus of the work is on IPC based on open-cell foams impregnated with an epoxy resin. Attention is paid first to a soft polymer foam, to investigate the influence of the epoxy formulation, with different amounts of a thermal initiator and a photoinitiator, on the front propagation features and total process time. An optimal formulation, with limited thermal degradation is identified, and is applied to produce an ICP based on an aluminum open-cell foam template.

2. EXPERIMENTAL

2.1. Materials and processes

In this study a cycloaliphatic epoxy was used as the photocurable resin (3-4-epoxycyclohexane methyl3'-4'-epoxycyclohexyl-carboxylate, Omnilane OC 1005, IGM, Italy), with a molecular weight of 232.32 g/mol and a functionality of 2. The photoinitiator and thermal initiators were respectively p-(octyloxyphenyl)-phenyliodonium hexafluoroantimonate (IOC8SbF6, ABCR, Germany) and 1,1,2,2-Tetraphenyl-1,2-ethanediol (TPED 98%, Acros, USA) and were used as received. A total of 9 formulations listed in Table 1 were prepared by adding the two types of initiators with different concentrations in the range from 0 to 3 wt% and stirred at 40°C for approximately 40 min. Two different open-cell foams were selected. The first was a soft polyurethane foam (Supercell 2017 EUROFOAM, EUROSPUMA, Portugal) with a density of 20 kg/m^3, and a typical pore diameter of 100 μm. This foam was selected according to its ability to be squeezed easily in order to facilitate the resin impregnation. Cylindrical foam samples with a height of 15 mm and a diameter of 16 mm were immersed into the formulations in a compressed state and then let expand back to their original dimensions to enable impregnation by the liquid resin. The second was an aluminum foam with a typical pore diameter of 500 μm produced at the Laboratory for Mechanical Metallurgy at the EPFL, in the form of cylinders with a height of 25 mm and a diameter of 30 mm. Since the aluminum foam could not be squeezed to favor resin impregnation, the formulation (with 1%wt of both initiators) was poured into a silicon mold with same diameter as the foam sample until half of it was filled and then the foam sample was pushed into the mold in order to impregnate the bottom half. Then, additional formulation was poured into the mold in order to impregnate the upper half of the foam sample. Notice that a simple vacuum infiltration process can be used as an alternative.

The impregnated polymer foam samples were placed on an aluminum foil to eliminate excess resin and subsequently placed on a support for direct UV irradiation at 40 mW/cm^2 on their upper surface. The UV source was a 200 W high-pressure mercury lamp (OmniCure 2000, EXFO, Canada) equipped with a liquid lightguide and a collimator to ensure homogeneous light intensity over the whole upper surface of the impregnated foam samples. The light intensity was measured using a calibrated radiometer (Silver Line, CON-TROL-CURE,

Germany), between 230 and 410 nm. The light was turned off when the front started to propagate.

Table 1: Composition of the investigated formulations.

#	IOC8 SbF6	TPED
1.	0,5 %wt	0 %wt
2.	1 %wt	0 %wt
3.	2 %wt	0 %wt
4.	3 %wt	0 %wt
5.	0,5 %wt	0,5 %wt
6.	0,5 %wt	1,5 %wt
7.	0,5 %wt	3 %wt
8.	1,5 %wt	0,5 %wt
9.	3 %wt	0,5 %wt

2.2. Characterization of the frontal polymerization

An infrared thermal camera (T450sc, FLIR, France) was used to monitor the propagation of the polymerization front. The experiments were carried out in ambient conditions (approximately 20°C). The camera was placed at a distance of 22.5 cm from the side of the samples to acquire in real-time the thermal field on the lateral surface of the impregnated foam (Figure 1). In order to characterize the behavior of the propagating polymerization front, four different parameters were considered: starting time of the front, t_{start}, front velocity, V_f, maximum temperature, T_{max}, and process time, $t_{process}$, sum of the time t_{start} and propagation time $t_{propagation} = H/V_f$, where H is the height of the foam sample. The temperature of three different points along the height of the samples was recorded at a rate of 1 frame/s: sp1 at the upper surface, where the front should initiate; sp2, 5 mm below sp1, where a stable propagating front should be ongoing; sp3, 5 mm below sp2, where the polymerization front should pass with the same condition as in sp2. For each formulation, three samples were tested. The frontal propagation was also recorded for formulation #5 using a conventional camera, and a sequence of photographs is reported in the Supplementary Information.

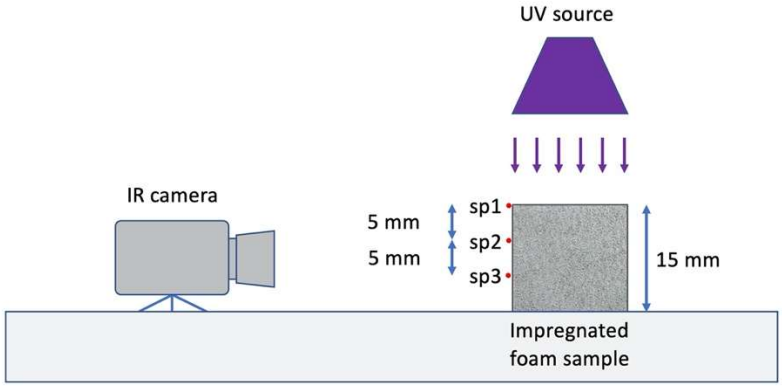

Figure 1. Sketch of the experimental setup to characterize the frontal propagation. See text for details.

The starting time represents the initiation of the thermal polymerization front, which is expected to occur on the top irradiated surface of the sample. It was determined as the time after the onset of UV irradiation, when the top of the foam sample locally reached a temperature of 250°C. It turned out that for all samples, the point where this occurred was located below the top surface, in the space between sp1 and sp2, due to the required thermal mass for the FP process as discussed in the following. The light was switched off at the starting time because the front propagated independently from the UV radiation. The front propagation velocity was calculated using the recorded videos, from the time taken by the front (temperature between 250°C and 270°C or higher) to travel between sp2 and sp3. The maximum temperature was directly obtained from the thermal field images. The process time was eventually calculated from the staring time and front propagation at constant velocity throughout the sample height (15 mm). The front behavior was characterized by a good level of homogeneity between sp2 and sp3. This created the conditions to measure the front velocity with a good precision using computation and image mapping on the video frames. Figure 2 shows the result of the front propagation experiment for formulation #7. The shape of the temperature vs. time curves is a clear manifestation that a frontal polymerization occurred, represented by a thermal wave that passes the recording points. These types of curves were observed for all investigated compositions (data in Supplementary Information).

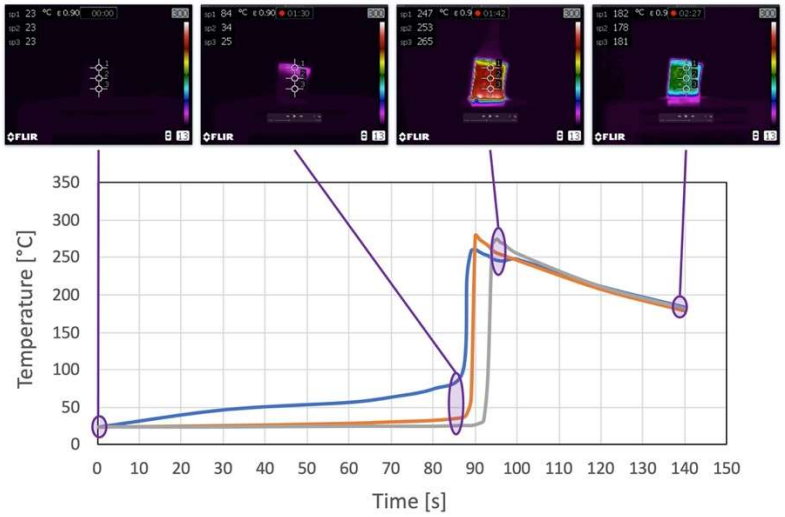

Figure 2. Example of a frontal polymerization experiment for formulation #7. The thermal images include the position of the points sp1, sp2 and sp3 shown with open white dots within the 10 mm x 15 mm studied region and the temperature vs. time curves recorded at the different positions (sp1: blue; sp2: orange; sp3: grey). The UV light was turned on at time 0s, and switched off at 86 s.

2.3. Characterization methods

Thermogravimetric analysis (TGA 4000, Perkin Elmer) was conducted in order to investigate degradation phenomena of the non-impregnated foam and the resin with and without initiators. Samples of few mg were heated under air at 10°C/min from 30°C to 500°C. Morphological characterizations were performed using a scanning electron microscope (SEM, TM-1000, Hitachi) and a numerical optical microscope (VHX-5000, Keyence). A study on the efficiency of the photo-induced section of the process was conducted by means of photo-differential scanning calorimetry (photo-DSC, Q100 from TA instruments equipped with the same UV source as for the frontal polymerization experiments). For the analysis, about 8.5 mg of the formulations were weighted and placed in an open aluminum pan with an empty open aluminum pan as a reference. The light intensity was 40 mW/cm^2 and the test duration was set to 200 s to ensure that the polymerization reaction was completed. The same experiment was repeated on the cured sample in order to obtain the baseline heat flow, that was subtracted to the first thermogram. DSC analysis of samples taken at a depth of 1 cm from the top surface of the cured foam samples was carried out with the same DSC equipment. Experiments were conducted in two subsequent scans from 0°C to 200°C with a heating rate of 20°C/min. The first scan enabled to detect the presence of exothermic peaks as a signature of a possible incomplete reaction whereas the second scan enabled to check if the reaction was complete.

3. RESULTS AND DISCUSSION

The PU foam was impregnated with the different epoxy formulations and UV irradiated from the top. The efficiency of the front propagation was investigated in the impregnated foams in order to design the best epoxy-based formulation in term of photoinitiator and thermal initiator content. It was first checked that adding both types of initiators to the formulation was necessary to initiate, and then propagate the front. For instance no propagation was observed when the thermal initiator TPED was absent (i.e., formulations #1, 2, 3 and 4).

3.1. Starting time and kinetics of the propagating front

Influence of photoinitiator

Figure 3 shows the starting time and front velocity of impregnated formulations as a function of IOC8SbF6 photoinitiator content keeping the thermal initiator TPED at a concentration of 0.5 wt%. It is evident that increasing the photoinitiator content from 0.5 wt% to 1.5 wt% reduced the starting time due to a higher content of photogenerated reactive species. On the other hand, when the photoinitiator was further increased to a content of 3 wt% the starting time slightly increased. This could be attributed to an internal filter effect due to the production of secondary aromatic species photogenerated by the iodonium salt itself, that absorb at the same wavelength as the photoinitiator, limiting the possibility of producing new reactive species [14–16]. As a result, a large enhancement of the front velocity was measured by increasing the photoinitiator content, with a plateau reached for 1.5 wt% of IOC8SbF6.

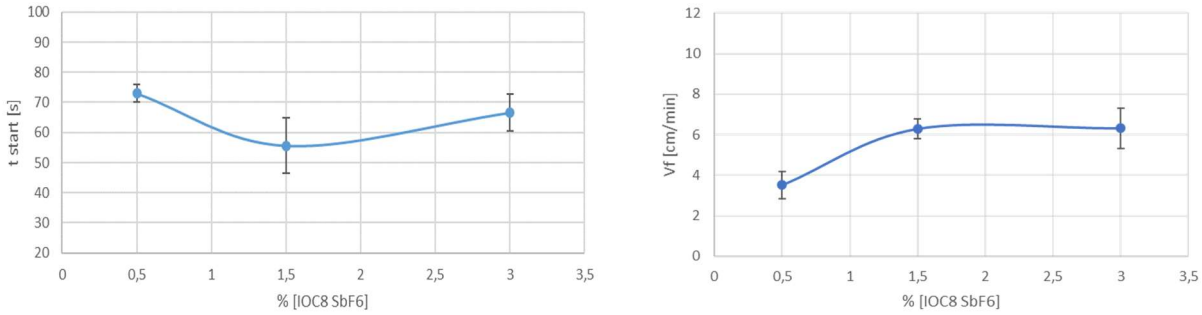

Figure 3. Starting time (t_{start}, left) and front velocity (V_f, right) of the thermal front measured as a function of photoinitiator concentration (the thermal initiator is kept at 0.5 wt%).

Influence of thermal initiator

Figure 4 shows the starting time and front velocity of impregnated formulations as a function of thermal initiator content keeping the photoinitiator at a concentration of 0.5 wt%. Here, it is evident that the front velocity was enhanced by increasing the thermal initiator content, however with a concomitant increase of starting time. The starting time is related to the photo-activity of the formulation, and the recorded increase can be related to a competitive screening effect of the thermal initiator with respect to the cationic photoinitiator. In fact, the UV-absorption of the thermal initiator overlaps that of the cationic photoinitiator [17], and this competitive effect decreases the photon availability for IOC8SbF6, thus reducing the generation of photoreactive species, hence increasing the polymerization starting time. On the other hand, the front velocity is a thermal phenomenon and therefore was enhanced by the increase of the thermal initiator.

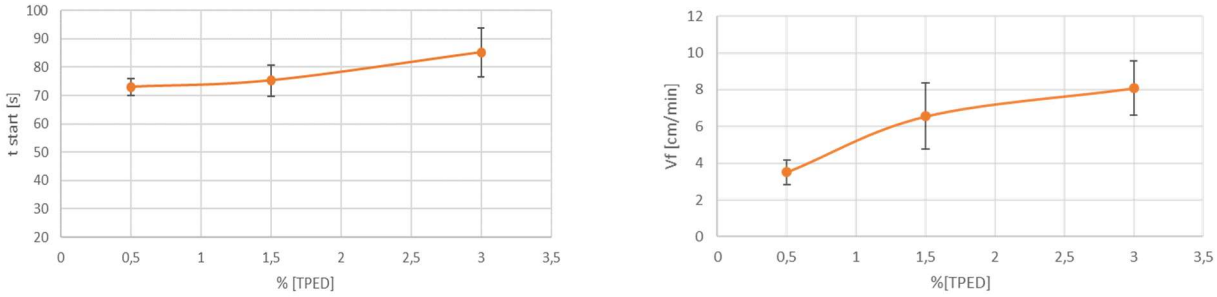

Figure 4. Starting time (t_{start}, left) and front velocity (V_f, right) for the thermal front measured as a function of thermal initiator concentration (the photoinitiator is kept at 0.5 wt%).

3.2. Efficiency of the photoinduced section of the RICFP process

The efficiency of the photo-induced section of the RICFP process was investigated through photo-DSC measurements. The theoretical enthalpy of the reaction, H_{th}, was determined to be 749.05 J/g through the equation:

$$H_{th} = \frac{f E_a}{M_w} \qquad [1]$$

where $f = 2$ and $M_w = 252.32$ g/mol are the functionality and molecular weight of the epoxy monomer, respectively, and $E_a = 94.5$ kJ/mol is the theoretical enthalpy for a single reacted epoxide group [18]. The conversion rate, $\dot{\alpha}$, was calculated by fitting the autocatalytic model to the experimental data [19].

Influence of photoinitiator

The conversion rate as a function of photoinitiator content is reported for formulations containing 0.5 wt% of TPED in Figure 5 (blue curve), and compared with the conversion rate for formulations without any thermal initiator (red curve). In the latter case, a large increase of the conversion rate with increasing photoinitiator is evident up to a concentration of 1 wt%, above which the conversion rate decreased. This is explained on the basis of an internal filter effect as previously discussed. This effect becomes more critical when the percentage of photoinitiator is between 1.5 wt% and 3 wt% leading to a drastic loss of efficiency of the photo-induced process. Interestingly, when 0.5 wt% thermal initiator was present, the conversion rate continuously decreased with increasing photoinitiator. The large difference observed at the lowest investigated concentration of photoinitiator reflects an important acceleration upon adding the thermal initiator.

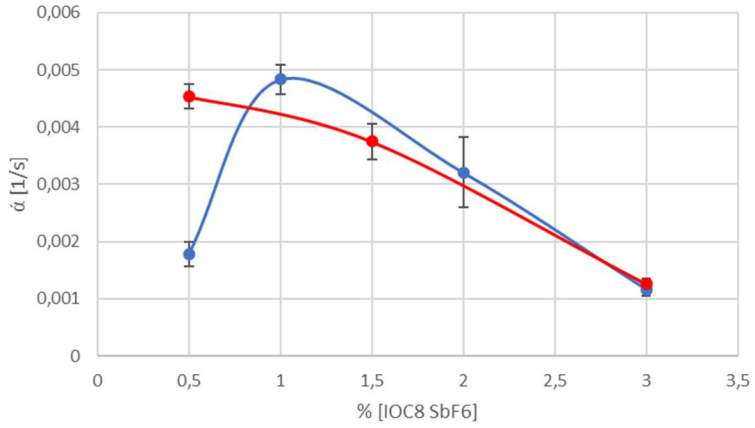

Figure 5. Conversion rate as a function of photoinitiator content for epoxy formulations containing 0.5 wt% of TPED (blue curve) and for the same epoxy formulations without thermal initiator (red curve).

Influence of thermal initiator

Figure 6 shows the conversion rate as a function of thermal initiator content for formulations containing 0.5 wt% of cationic photoinitiator. The addition of 0.5 wt% of TPED greatly increased the conversion rate. This could probably be attributed to the radical induced cationic frontal polymerization due to the radicals generated by the thermal initiator and oxidized to carbocation by the iodonium salt. This photoredox process enhanced the amount of carbocationic reactive species, increasing the rate of epoxy ring-opening polymerization reaction. Then, by further increasing TPED it is possible to observe a slightly reduced

polymerization rate. Again, this could be due to a competitive light absorption by the thermal initiator given the presence of chromophore groups within its structure. This condition has led to a similar loss of efficiency of the photo-induced section of the process at different amount of thermal initiator and, therefore, to a delay in the starting time of the polymerization front.

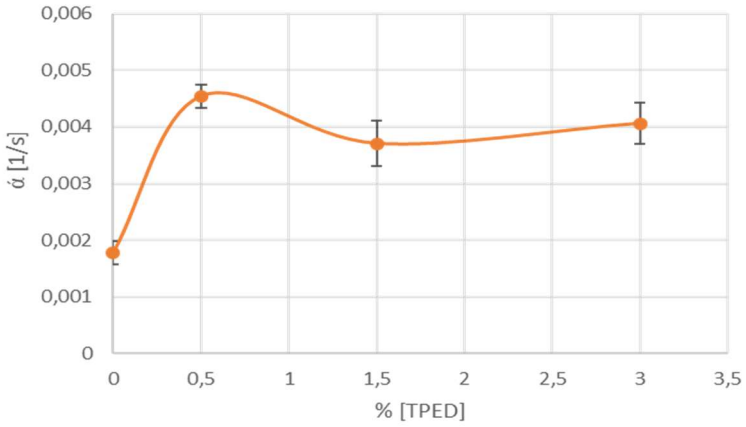

Figure 6. Conversion rate as a function of thermal initiator content for epoxy formulations containing 0.5 wt% of IOC8SbF6.

3.3. Process time optimization

The detailed data from the DSC analysis are reported in the Supplementary Information. It was found that the conversion of the resin cured in the impregnated foam was above 99% for all investigated compositions, so that the total reaction time was long enough to ensure complete conversion. Figure 7 shows the influence of both types of initiators on process time (starting time + propagation time across the 15 mm sample) for foams impregnated with epoxy formulations, containing either a constant thermal initiator and varying the photoinitiator between 0.5 wt% up to 3 wt% or vice versa. The process time was comprised between 60 s and 100 s for the investigated formulations. It decreased with increasing cationic photoinitiator from 0.5 wt% up to 1.5 wt%, due to the combined decrease of the starting time of the front and increase of the front velocity (Figure 3). In contrast, the amount of thermal initiator TPED did not affect the process time. In that case, the increase of the front velocity was offset by the increase of the starting time (Figure 4).

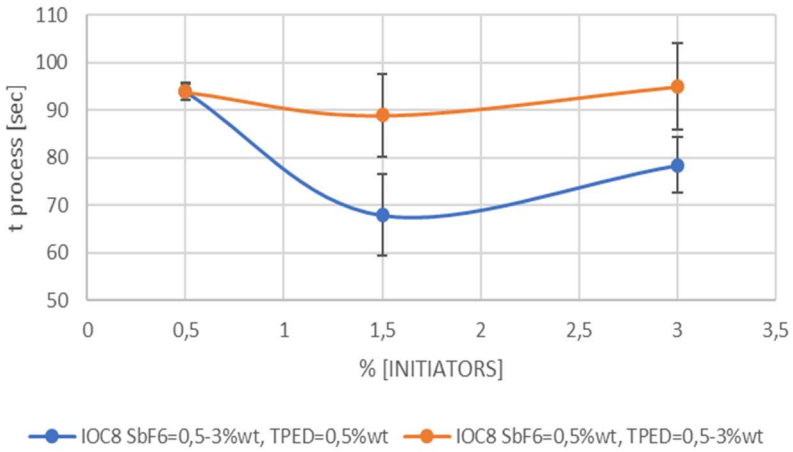

Figure 7. Influence of composition on process time for 15 mm thick impregnated foams.

3.4. Maximum temperature reached and degradation phenomena

The maximum temperature reached during front propagation is reported in Figure 8 for the epoxy formulations as a function of photoinitiator content (keeping the same amount of thermal initiator) and thermal initiator content (keeping the same amount of photoinitiator). By increasing the photoinitiator content a linear increase of exothermicity was measured, reaching a peak above 300°C for the formulation containing 3 wt% of the photoinitiator. Regarding the effect of the thermal initiator a maximum value of temperature is recorded at 1.5%wt, with a peak at around 290°C.

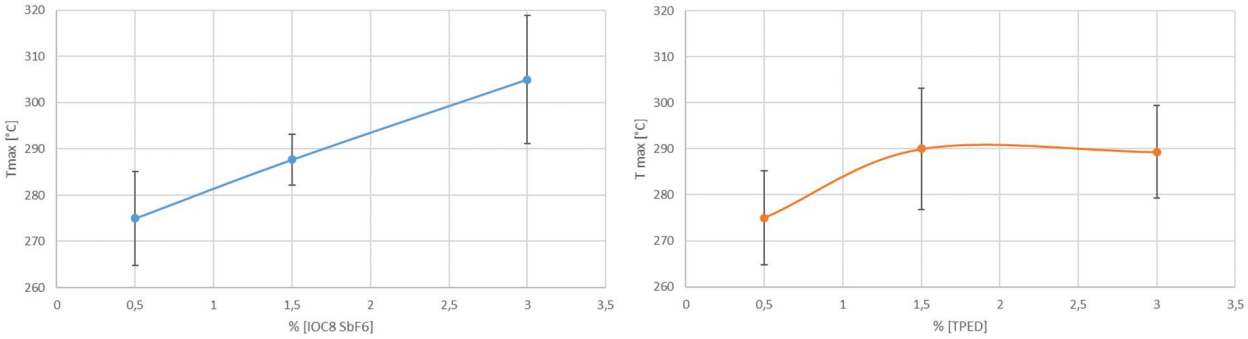

Figure 8. Maximum temperature for the epoxy formulations a as a function of photoinitiator content keeping the TPED at 0.5 wt% (left curve) or as a function of thermal initiator content keeping the IOC8SbF6 at 0.5 wt% (right curve).

Such high temperatures reached during the frontal propagation could induce some degradation of the epoxy and of the polyurethane foam. The TGA revealed that the onset and

peak degradation temperatures were 265°C and 283°C, respectively, for the foam, and 365°C and 411°C, respectively, for the epoxy with 0.5%wt of both types of initiators (data in Supplementary Information). This implies that the foam degraded during frontal propagation, as the temperatures were always greater than the foam degradation onset. However, the epoxy was stable in these conditions. To further examine this degradation issue, two limit formulations were selected, namely #5 (IOC8SbF6 = 0.5 wt%, TPED = 0.5 wt%, T_{max} = 275 ± 10°C) and #9 (IOC8 SbF6 = 3 wt%, TPED = 0.5 wt%, T_{max} = 305 ± 14°C). The optical micrographs reported in Figure 9 show a large difference in color, from yellow for the foam impregnated with formulation #5, to dark brown for the foam impregnated with formulation #9. The difference in color is present throughout the entire structure of the sample, a symptom of greater induced degradation in the system when a higher maximum temperature is reached. The electron micrographs also shown in Figure 9 reveal that the foam impregnated with formulation #5 had a homogeneous structure with smooth interface between the epoxy and the polyurethane. A large amount of porosity is also evident. This effect was in fact essentially due to the formation of gasses during the front propagation since the boiling temperature of the resin (170°C) was exceeded [5]. A complete disintegration of the structure is clearly visible in the foam impregnated with formulation #9, a result of severe thermally-induced degradation.

In order to reduce the thermal degradation issue, one could use other epoxies such as bisphenol-A diglycidyl ether (BADGE), leading to maximum temperatures below 210°C with the same initiator system as used in the present work [20]. A further benefit of BADGE resins is their high boiling point of 487°C, which would prevent boiling to occur. Notice that potential drawbacks with such epoxies are their toxicity and high viscosity, which would in turn complicate the impregnation step.

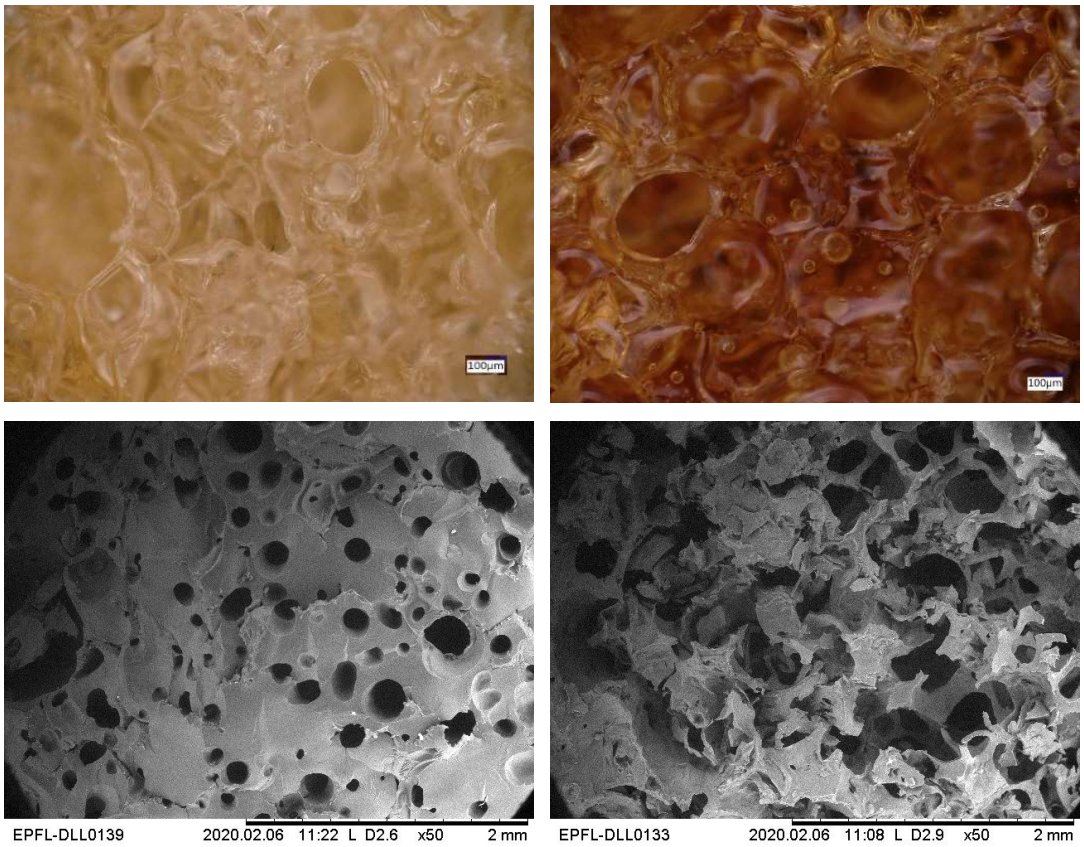

Figure 9. Optical micrographs of cured foams impregnated with formulation #5 (top left) and with formulation #9 (top right) and scanning electron micrographs taken at deeper layers from the surface of cured foam impregnated with formulation #5 (bottom left) and with formulation #9 (bottom right).

3.6. RICFP in aluminum foam

An Al-epoxy ICP was produced using the RICFP process. The non-impregnated Al foam and the final cured Al-epoxy ICP samples are shown in Figure 10. A first attempt, with the light source placed close to the top surface of the impregnated aluminum foam failed to generate a propagation front. Only a superficial cure was achieved, to a depth of approximately 5 mm (white line in the Figure). The reason is that a critical thickness, where light intensity is high enough, is required to trigger the RICFP. This critical thickness corresponds to a critical mass of resin, below which the generated heat would dissipate, thereby inhibiting the front propagation. This was the case for the PU foam that was transparent enough to the UV light, and indeed the maximum temperature at propagation onset was a few mm below the irradiated surface, where heat could no longer dissipate. In contrast, this was not the case for the metal foam owing to high optical absorption and high thermal conductivity of the metal. To solve this problem, a 5 mm thick layer of liquid formulation was added on the top surface of the

impregnated foam. FP and full curing took place, however leading again to significant porosity within the cured epoxy due to the boiling of the liquid resin and production of gases. The mass of the additional resin layer, which would correspond to the critical mass was close to 4 g. This value will obviously depend on the specific thermal boundary conditions, i.e., an insulating foam structure in the present investigation.

Figure 10. Aluminum open-cell foam sample (diameter 3 cm, the white line indicates the thickness of the cured superficial layer in the first experiment), and interpenetrating phase composite based on the impregnated and cured epoxy within the aluminum foam.

4. CONCLUSIONS

IPC based on PU and Al open-cell foams impregnated with a cycloaliphatic epoxy formulation were produced using a RICFP process. The influence of photoinitiator and thermal initiator content on starting time, front velocity, process time and maximum temperature was systematically evaluated for the PU foam, in order to identify an optimal formulation in terms of exothermicity and process time. The propagating polymerization front was found to develop with a degree of conversion in deeper layers close to 100%, when the concentration of both photoinitiator and thermal initiator was greater than 0.5 wt%. The optimal concentrations of initiators were between 0.5 and 1.5 wt% for the cationic photoinitiator and 0.5 wt% for the thermal initiator. The process time to fully cure the 15 mm thick samples was close to 80 s, with limited influence of the amount of initiators. The maximum temperature reached by the propagation front was in the range 275°C-305°C, and essentially increased with the amount of photoinitiator. This large temperature increase provoked the boiling of the liquid epoxy and consecutive formation of pores in the polymer phase, and degraded the polymer foam but not the metal foam. A critical resin thickness of few mm, which corresponded to a critical mass of few g to trigger the front propagation in the open-cell foam structure was also uncovered.

ACKNOWLEDGEMENTS

The authors are indebted to the Mobility Program Fellowship of the Politecnico di Torino for the financial support provided to DM for his stay at the EPFL. They also acknowledge the Laboratory of Photonic Materials and Fibre Devices (FIMAP-EPFL) for the loan of the IR camera, the Laboratory for Mechanical Metallurgy (LMM-EPFL) for the aluminum foam samples, the Discovery Learning Laboratories (DLL-EPFL) for access to their optical and scanning electron microscopes and Molecular and Hybrid Materials Characterization Center (MHMC-EPFL) for access to their TGA instrument.

REFERENCES

1. Wegner L.D., Gibson L.J., *Int. J. Mech. Sci.* **42***:* 925–942 (2000).
2. Angamnuaysiri K., Asavavisithchai S., *Mater. Test.* **60**: 453–457 (2018).
3. Liu J., Chen C., Huang K., Yan Y., Zhang C., Jia S., *Mater. Res. Express* **6**: 1165c8 (2019).
4. Liu S., Li A., *Compos. Struct.* **203**: 18–29 (2018).
5. Sangermano M., D'Anna A., Marro C., Klikovits N., Liska R., *Compos. Part B Eng.* **143**: 168–171 (2018).
6. Sangermano M., Antonazzo I., Sisca L., Carello M., *Polym. Int.* **68**: 1662–1665 (2019).
7. Bomze D., Knaack P., Liska R., *Polym. Chem.* **6**: 8161–8167 (2015).
8. Klikovits N., Liska R., D'Anna A., Sangermano M., *Macromol. Chem. Phys.* **218**: 1700313 (2017).
9. Nason C., Roper T., Hoyl, C., Pojman J.A., *Macromolecules* **38**: 5506–5512 (2005).
10. Mariani A., Bidali S., Fiori S., Sangermano M., Malucelli G., Bongiovanni R., Priola A., *J. Polym. Sci. Part A. Polym. Chem.* **42**: 2066–2072, (2004).
11. Pojman, J.A. *Frontal Polymerization*; Elsevier, Amsterdam, Vol. 4, p. 980 (2012).
12. Pojman J.A., Ilyashenko V.M., Khan A.M., *J. Chem. Soc. Faraday Trans.* **92**: 2824–2836 (1996).
13. Knaack P., Klikovits N., Tran A.D., Bomze D., Liska R., *J. Polym. Sci. Part Polym. Chem.* **57**: 1155–1159 (2019).
14. Maurizio, F.; Stefano, P.; Davide, R. *Photoorganocatalysis In Organic Synthesis*; Catalytic Science Series; World Scientific Publishing Company, Singapore, 2019.
15. Kabatc J., Ortyl J., Kostrzewska K., *RSC Adv.* **7**: 41619–41629 (2017)

16. Abadie M.J.M., Chia N.K., Boey F., *J. Appl. Polym. Sci.* **86**: 1587–1591 (2002).
17. Potey L.C., Kosalge S.B., Sarode R.S., *Int. J. Pharm. Drug Anal.* **2**: 55–58 (2014).
18. Brandrup, J.; Immergut, E.H.; Grulke, A. *Polymer Handbook, 4th ed.*; Wiley, New York, (1999).
19. Dalle Vacche S., Geiser V., Leterrier Y., Manson J.A.E., *Polymer* **51**: 334–341 (2010).
20. Bomze D., Knaack P., Koch T., Jin H., Liska R., *J. Polym. Sci. Part A Polym. Chem.* **54**: 3751–3759 (2016).